

Photonic Events with Large Missing Energy in e^+e^- Collisions at $\sqrt{s} = 161$ GeV

The OPAL Collaboration

Abstract

Photonic events with large missing energy have been observed with the OPAL detector at LEP using two search topologies. The first topology looks for events with significant missing energy and at least one photon in $|\cos\theta| < 0.7$ with large scaled energy, $x_\gamma > 0.2$. The second topology looks for events with an acoplanar photon pair where both photons are in $|\cos\theta| < 0.7$ and have energy exceeding 1.75 GeV. In the data sample corresponding to an integrated luminosity of 10.0 pb^{-1} , 11 events are selected for the first topology and a cross-section of $1.6 \pm 0.5 \text{ pb}$ is measured within the kinematic acceptance, consistent with that expected for the Standard Model process $e^+e^- \rightarrow \nu\bar{\nu}\gamma(\gamma)$. No events are selected for the second topology giving a 95% CL cross-section upper limit of 0.41 pb within the kinematic acceptance. Upper limits on the cross-section times branching ratio for new particle production are also derived.

Submitted to Physics Letters B

The OPAL Collaboration

K. Ackerstaff⁸, G. Alexander²³, J. Allison¹⁶, N. Altekamp⁵, K. Ametewee²⁵, K.J. Anderson⁹, S. Anderson¹², S. Arcelli², S. Asai²⁴, D. Axen²⁹, G. Azuelos^{18,a}, A.H. Ball¹⁷, E. Barberio⁸, R.J. Barlow¹⁶, R. Bartoldus³, J.R. Batley⁵, J. Bechtluft¹⁴, C. Beeston¹⁶, T. Behnke⁸, A.N. Bell¹, K.W. Bell²⁰, G. Bella²³, S. Bentvelsen⁸, P. Berlich¹⁰, S. Bethke¹⁴, O. Biebel¹⁴, V. Blobel²⁷, I.J. Bloodworth¹, J.E. Bloomer¹, M. Bobinski¹⁰, P. Bock¹¹, H.M. Bosch¹¹, M. Boutemour³⁴, B.T. Bouwens¹², S. Braibant¹², R.M. Brown²⁰, A. Buguzzi², H.J. Burckhart⁸, C. Burgard⁸, R. Bürgin¹⁰, P. Capiluppi², R.K. Carnegie⁶, A.A. Carter¹³, J.R. Carter⁵, C.Y. Chang¹⁷, D.G. Charlton^{1,b}, D. Chrisman⁴, P.E.L. Clarke¹⁵, I. Cohen²³, J.E. Conboy¹⁵, O.C. Cooke¹⁶, M. Cuffiani², S. Dado²², C. Dallapiccola¹⁷, G.M. Dallavalle², S. De Jong¹², L.A. del Pozo⁸, K. Desch³, M.S. Dixit⁷, E. do Couto e Silva¹², M. Doucet¹⁸, E. Duchovni²⁶, G. Duckeck³⁴, I.P. Duerdoth¹⁶, J.E.G. Edwards¹⁶, P.G. Estabrooks⁶, H.G. Evans⁹, M. Evans¹³, F. Fabbri², P. Fath¹¹, F. Fiedler²⁷, M. Fierro², H.M. Fischer³, R. Folman²⁶, D.G. Fong¹⁷, M. Foucher¹⁷, A. Fürtjes⁸, P. Gagnon⁷, J.W. Gary⁴, J. Gascon¹⁸, S.M. Gascon-Shotkin¹⁷, N.I. Geddes²⁰, C. Geich-Gimbel³, T. Gerasis²⁰, G. Giacomelli², P. Giacomelli⁴, R. Giacomelli², V. Gibson⁵, W.R. Gibson¹³, D.M. Gingrich^{30,a}, D. Glenzinski⁹, J. Goldberg²², M.J. Goodrick⁵, W. Gorn⁴, C. Grandi², E. Gross²⁶, J. Grunhaus²³, M. Gruwé⁸, C. Hajdu³², G.G. Hanson¹², M. Hansroul⁸, M. Hapke¹³, C.K. Hargrove⁷, P.A. Hart⁹, C. Hartmann³, M. Hauschild⁸, C.M. Hawkes⁵, R. Hawkings⁸, R.J. Hemingway⁶, M. Herndon¹⁷, G. Herten¹⁰, R.D. Heuer⁸, M.D. Hildreth⁸, J.C. Hill⁵, S.J. Hillier¹, T. Hilse¹⁰, P.R. Hobson²⁵, R.J. Homer¹, A.K. Honma^{28,a}, D. Horváth^{32,c}, R. Howard²⁹, R.E. Hughes-Jones¹⁶, D.E. Hutchcroft⁵, P. Igo-Kemenes¹¹, D.C. Imrie²⁵, M.R. Ingram¹⁶, K. Ishii²⁴, A. Jawahery¹⁷, P.W. Jeffreys²⁰, H. Jeremie¹⁸, M. Jimack¹, A. Joly¹⁸, C.R. Jones⁵, G. Jones¹⁶, M. Jones⁶, R.W.L. Jones⁸, U. Jost¹¹, P. Jovanovic¹, T.R. Junk⁸, D. Karlen⁶, K. Kawagoe²⁴, T. Kawamoto²⁴, R.K. Keeler²⁸, R.G. Kellogg¹⁷, B.W. Kennedy²⁰, B.J. King⁸, J. Kirk²⁹, S. Kluth⁸, T. Kobayashi²⁴, M. Kobel¹⁰, D.S. Koetke⁶, T.P. Kokott³, M. Kolrep¹⁰, S. Komamiya²⁴, T. Kress¹¹, P. Krieger⁶, J. von Krogh¹¹, P. Kyberd¹³, G.D. Lafferty¹⁶, R. Lahmann¹⁷, W.P. Lai¹⁹, D. Lanske¹⁴, J. Lauber¹⁵, S.R. Lautenschlager³¹, J.G. Layter⁴, D. Lazic²², A.M. Lee³¹, E. Lefebvre¹⁸, D. Lellouch²⁶, J. Letts², L. Levinson²⁶, C. Lewis¹⁵, S.L. Lloyd¹³, F.K. Loebinger¹⁶, G.D. Long¹⁷, M.J. Losty⁷, J. Ludwig¹⁰, M. Mannelli⁸, S. Marcellini², C. Markus³, A.J. Martin¹³, J.P. Martin¹⁸, G. Martinez¹⁷, T. Mashimo²⁴, W. Matthews²⁵, P. Mättig³, W.J. McDonald³⁰, J. McKenna²⁹, E.A. Mckigney¹⁵, T.J. McMahon¹, A.I. McNab¹³, R.A. McPherson⁸, F. Meijers⁸, S. Menke³, F.S. Merritt⁹, H. Mes⁷, J. Meyer²⁷, A. Michelini², G. Mikenberg²⁶, D.J. Miller¹⁵, R. Mir²⁶, W. Mohr¹⁰, A. Montanari², T. Mori²⁴, M. Morii²⁴, U. Müller³, K. Nagai²⁶, I. Nakamura²⁴, H.A. Neal⁸, B. Nellen³, B. Nijhar¹⁶, R. Nisius⁸, S.W. O'Neale¹, F.G. Oakham⁷, F. Odorici², H.O. Ogren¹², N.J. Oldershaw¹⁶, T. Omori²⁴, M.J. Oreglia⁹, S. Orito²⁴, J. Pálincás^{33,d}, G. Pásztor³², J.R. Pater¹⁶, G.N. Patrick²⁰, J. Patt¹⁰, M.J. Pearce¹, S. Petzold²⁷, P. Pfeifenschneider¹⁴, J.E. Pilcher⁹, J. Pinfold³⁰, D.E. Plane⁸, P. Poffenberger²⁸, B. Poli², A. Posthaus³, H. Przysieznik³⁰, D.L. Rees¹, D. Rigby¹, S. Robertson²⁸, S.A. Robins¹³, N. Rodning³⁰, J.M. Roney²⁸, A. Rooke¹⁵, E. Ros⁸, A.M. Rossi², M. Rosvick²⁸, P. Routenburg³⁰, Y. Rozen²², K. Runge¹⁰, O. Runolfsson⁸, U. Ruppel¹⁴, D.R. Rust¹², R. Rylko²⁵, K. Sachs¹⁰, E.K.G. Sarkisyan²³, M. Sasaki²⁴, C. Sbarra², A.D. Schaille³⁴, O. Schaille³⁴, F. Scharf³, P. Scharff-Hansen⁸, P. Schenk²⁷, B. Schmitt⁸, S. Schmitt¹¹, M. Schröder⁸, H.C. Schultz-Coulon¹⁰, M. Schulz⁸, M. Schumacher³, P. Schütz³, W.G. Scott²⁰, T.G. Shears¹⁶, B.C. Shen⁴, C.H. Shepherd-Themistocleous⁸, P. Sherwood¹⁵, G.P. Siroti², A. Sittler²⁷, A. Skillman¹⁵, A. Skuja¹⁷, A.M. Smith⁸, T.J. Smith²⁸, G.A. Snow¹⁷, R. Sobie²⁸, S. Söldner-Rembold¹⁰, R.W. Springer³⁰, M. Sproston²⁰, A. Stahl³, M. Steiert¹¹, K. Stephens¹⁶, J. Steuerer²⁷, B. Stockhausen³, D. Strom¹⁹, F. Strumia⁸, P. Szymanski²⁰, R. Tafirout¹⁸, S.D. Talbot¹, S. Tanaka²⁴, P. Taras¹⁸, S. Tarem²², M. Thiergen¹⁰, M.A. Thomson⁸, E. von Törne³, S. Towers⁶, I. Trigger¹⁸, T. Tsukamoto²⁴, E. Tsur²³, A.S. Turcot⁹, M.F. Turner-Watson⁸, P. Utzat¹¹, R. Van Kooten¹², M. Verzocchi¹⁰, P. Vikas¹⁸, M. Vincter²⁸, E.H. Vokurka¹⁶, F. Wackerle¹⁰, A. Wagner²⁷, C.P. Ward⁵,

D.R. Ward⁵, J.J. Ward¹⁵, P.M. Watkins¹, A.T. Watson¹, N.K. Watson⁷, P.S. Wells⁸, N. Wermes³,
J.S. White²⁸, B. Wilkens¹⁰, G.W. Wilson²⁷, J.A. Wilson¹, G. Wolf²⁶, S. Wotton⁵, T.R. Wyatt¹⁶,
S. Yamashita²⁴, G. Yekutieli²⁶, V. Zacek¹⁸,

¹School of Physics and Space Research, University of Birmingham, Birmingham B15 2TT, UK

²Dipartimento di Fisica dell' Università di Bologna and INFN, I-40126 Bologna, Italy

³Physikalisches Institut, Universität Bonn, D-53115 Bonn, Germany

⁴Department of Physics, University of California, Riverside CA 92521, USA

⁵Cavendish Laboratory, Cambridge CB3 0HE, UK

⁶Ottawa-Carleton Institute for Physics, Department of Physics, Carleton University, Ottawa, Ontario K1S 5B6, Canada

⁷Centre for Research in Particle Physics, Carleton University, Ottawa, Ontario K1S 5B6, Canada

⁸CERN, European Organisation for Particle Physics, CH-1211 Geneva 23, Switzerland

⁹Enrico Fermi Institute and Department of Physics, University of Chicago, Chicago IL 60637, USA

¹⁰Fakultät für Physik, Albert Ludwigs Universität, D-79104 Freiburg, Germany

¹¹Physikalisches Institut, Universität Heidelberg, D-69120 Heidelberg, Germany

¹²Indiana University, Department of Physics, Swain Hall West 117, Bloomington IN 47405, USA

¹³Queen Mary and Westfield College, University of London, London E1 4NS, UK

¹⁴Technische Hochschule Aachen, III Physikalisches Institut, Sommerfeldstrasse 26-28, D-52056 Aachen, Germany

¹⁵University College London, London WC1E 6BT, UK

¹⁶Department of Physics, Schuster Laboratory, The University, Manchester M13 9PL, UK

¹⁷Department of Physics, University of Maryland, College Park, MD 20742, USA

¹⁸Laboratoire de Physique Nucléaire, Université de Montréal, Montréal, Quebec H3C 3J7, Canada

¹⁹University of Oregon, Department of Physics, Eugene OR 97403, USA

²⁰Rutherford Appleton Laboratory, Chilton, Didcot, Oxfordshire OX11 0QX, UK

²²Department of Physics, Technion-Israel Institute of Technology, Haifa 32000, Israel

²³Department of Physics and Astronomy, Tel Aviv University, Tel Aviv 69978, Israel

²⁴International Centre for Elementary Particle Physics and Department of Physics, University of Tokyo, Tokyo 113, and Kobe University, Kobe 657, Japan

²⁵Brunel University, Uxbridge, Middlesex UB8 3PH, UK

²⁶Particle Physics Department, Weizmann Institute of Science, Rehovot 76100, Israel

²⁷Universität Hamburg/DESY, II Institut für Experimental Physik, Notkestrasse 85, D-22607 Hamburg, Germany

²⁸University of Victoria, Department of Physics, P O Box 3055, Victoria BC V8W 3P6, Canada

²⁹University of British Columbia, Department of Physics, Vancouver BC V6T 1Z1, Canada

³⁰University of Alberta, Department of Physics, Edmonton AB T6G 2J1, Canada

³¹Duke University, Dept of Physics, Durham, NC 27708-0305, USA

³²Research Institute for Particle and Nuclear Physics, H-1525 Budapest, P O Box 49, Hungary

³³Institute of Nuclear Research, H-4001 Debrecen, P O Box 51, Hungary

³⁴Ludwigs-Maximilians-Universität München, Sektion Physik, Am Coulombwall 1, D-85748 Garching, Germany

^a and at TRIUMF, Vancouver, Canada V6T 2A3

^b and Royal Society University Research Fellow

^c and Institute of Nuclear Research, Debrecen, Hungary

^d and Department of Experimental Physics, Lajos Kossuth University, Debrecen, Hungary

1 Introduction

In this paper we describe a search for photonic events with large missing energy in e^+e^- collisions at $\sqrt{s} = 161$ GeV. This high centre-of-mass energy provides the opportunity to search for new phenomena in e^+e^- collisions at LEP. The analysed data sample corresponds to an integrated luminosity of 10.0 pb^{-1} . The event selections are essentially identical to those used for topologies A and B of the OPAL measurement of photonic events with missing energy performed at $\sqrt{s} = 130 - 140$ GeV [1]. Those results were also used to search for excited neutrinos with photonic decays at $\sqrt{s} = 130 - 140$ GeV [2].

Two different event topologies, A and B, are designed to select events with one or two photons and significant transverse momentum imbalance thus signalling the presence of at least one neutrino-like invisible particle which interacts only weakly with matter. The acceptance of each topology is defined in terms of the photon energy, E_γ , scaled by the beam energy, ($x_\gamma \equiv E_\gamma/E_{\text{beam}}$), and the photon polar angle, θ , defined with respect to the electron beam direction. The definitions of the topologies are as follows :

Topology A: One or two photons accompanied by invisible particle(s) ($e^+e^- \rightarrow \gamma(\gamma) + \text{invisible particle(s)}$). At least one photon with $x_\gamma > 0.2$ and $|\cos\theta| < 0.7$.

Topology B: Acoplanar photon pair ($e^+e^- \rightarrow \gamma\gamma + \text{invisible particle(s)}$). Two photons each with energy exceeding 1.75 GeV and $|\cos\theta| < 0.7$.

Topology A is sensitive to the production of one or two photons and missing energy, which within the Standard Model is expected from the $e^+e^- \rightarrow \nu\bar{\nu}\gamma(\gamma)$ process. Measurements of single photon production have been made in e^+e^- collisions at the Z^0 and at lower energies [3–5]. First results from centre-of-mass energies significantly above the Z^0 mass have also been reported [1, 6]. The expected visible energies are sufficiently large at the present centre-of-mass energies that doubly radiative neutrino production can lead to two photons being detected and therefore the experimental topology includes such cases. Topology A is also sensitive to several types of new physics in e^+e^- collisions (see e.g. [3, 7] and references therein). One type of new physics is $e^+e^- \rightarrow XY$ where X decays to $Y\gamma$ and Y is an invisible particle such as a neutrino or possibly a new particle that escapes detection. One example of this type of process is production of excited neutrinos, where in this case X is an excited neutrino and Y is a standard neutrino. Another example is production of neutralinos in supersymmetric theories, where in this case X is a heavier neutralino, for example $\tilde{\chi}_2^0$, and Y is the lightest neutralino, $\tilde{\chi}_1^0$, which is stable and escapes detection. The branching fraction for the radiative decay, $\tilde{\chi}_2^0 \rightarrow \tilde{\chi}_1^0\gamma$, may be small, but in some cases can be dominant [8]. Another type of new physics that could be seen in this search topology is the production of invisible particles made visible simply through initial state radiation.

Search topology B is designed for neutral events with an acoplanar photon pair and significant missing energy. This topology is sensitive to the production of two particles, one decaying invisibly and the other decaying into two photons. It is also sensitive to pair production of new neutral particles each of which undergoes radiative decay to an invisible particle, i.e. $e^+e^- \rightarrow XX$, $X \rightarrow Y\gamma$. Specifically regarding the latter possibility, the topology has acceptance for pair production of excited neutrinos ($X = \nu^*$, $Y = \nu$), and also for neutralino pair production ($X = \tilde{\chi}_2^0$, $Y = \tilde{\chi}_1^0$) for cases where particle X can decay radiatively. The latter scenario, with a substantial photonic branching ratio, is advocated in [9]. Also of interest are models with light gravitinos, \tilde{G} , with $X = \tilde{\chi}_1^0$, $Y = \tilde{G}$, where the photonic branching ratio is naturally large. Such a signature has been discussed in [10] and more recently in [11, 12]; cross-sections of order 1 pb are predicted at $\sqrt{s} = 161$ GeV for $M_{\tilde{\chi}_1^0} \approx 50$ GeV.

The acceptance of topology B overlaps partly with that of topology A but in this case the kinematic acceptance extends well below the $x_\gamma > 0.2$ requirement of topology A, thus allowing acceptance for

events with very low visible energy. However, a more restricted angular acceptance for the second photon is imposed to reduce the generally forward-peaked backgrounds. Both topologies are sensitive to doubly radiative neutrino production, $e^+e^- \rightarrow \nu\bar{\nu}\gamma\gamma$. This process is considered as part of the radiative correction of the inclusive single photon measurement in topology A, while for topology B, it represents the essentially irreducible Standard Model background to a search for new physics processes.

This paper will briefly describe the detector, the data sample and the Monte Carlo samples used. Then the event selection for each topology will be described, followed by the results and comparison to expected Standard Model contributions. Implications of these results on the possibility of new physics processes of the type $e^+e^- \rightarrow XX$ or XY , $X \rightarrow Y\gamma$ will be discussed. This analysis is particularly sensitive for the case $M_Y \approx 0$ which is relevant to excited neutrino ($X = \nu^*$, $Y = \nu$) production and to light gravitino ($X = \tilde{\chi}_1^0$, $Y = \tilde{G}$) hypotheses.

2 Detector, Data Sample and Monte Carlo Samples

The OPAL detector is described in detail elsewhere [13]. The measurements presented here are mainly based on the observation of clusters of energy deposited in the lead-glass electromagnetic calorimeters. These calorimeters together with the gamma-catcher calorimeter and forward detector provide a fully hermetic electromagnetic calorimeter down to polar angles of 60 mrad. The tracking system, consisting of a silicon microvertex detector, a vertex drift chamber and a large volume jet drift chamber, is used to select events consistent with zero charged particle multiplicity. Backgrounds from cosmic-ray interactions are removed using time-of-flight (TOF) information and the hadron calorimeter and muon detectors.

The data used in this analysis were recorded at an e^+e^- centre-of-mass energy of 161.3 ± 0.2 GeV, with an integrated luminosity of 10.0 pb^{-1} . The statistical error on the integrated luminosity is 0.4% and the systematic error is estimated to be 0.4%. The luminosity is determined from small angle Bhabha scattering events in the silicon-tungsten luminosity calorimeter. The Monte Carlo samples described below were all generated with a centre-of-mass energy of 161.0 GeV. The small difference in centre-of-mass energy between the Monte Carlo and data does not affect any results in this paper.

For the expected Standard Model signal process of $e^+e^- \rightarrow \nu\bar{\nu}\gamma(\gamma)$, the Monte Carlo generator NUNUGPV [14] was used. For the expected Standard Model background processes, we used a number of different generators: RADCOR [15] for $e^+e^- \rightarrow \gamma\gamma(\gamma)$; BHWIDE [16] and TEEGG [17] for $e^+e^- \rightarrow e^+e^-(\gamma)$; KORALZ [18] for $e^+e^- \rightarrow \mu^+\mu^-(\gamma)$ and $e^+e^- \rightarrow \tau^+\tau^-(\gamma)$; and the Vermaseren program [19] for leptonic final states from two-photon collisions.

To simulate possible new physics processes of the type $e^+e^- \rightarrow XY$ and $e^+e^- \rightarrow XX$ where X decays to $Y\gamma$ and Y escapes detection, the SUSYGEN [20] Monte Carlo generator was used. We produced neutralino pair events of the type $e^+e^- \rightarrow \tilde{\chi}_2^0\tilde{\chi}_1^0$ and $e^+e^- \rightarrow \tilde{\chi}_2^0\tilde{\chi}_2^0$, where $\tilde{\chi}_2^0 \rightarrow \tilde{\chi}_1^0\gamma$. Using the relatively flat angular distribution observed in the production of these generated events, the estimated efficiencies are generalised to the generic processes (replacing $\tilde{\chi}_2^0$ with X and $\tilde{\chi}_1^0$ with Y), assuming an isotropic angular distribution for XY and XX production and for X decay. For this paper we used samples of XY production with M_X from 80 to 160 GeV and with $M_Y = 0$. For XX production we analysed samples with M_X from 45 to 80 GeV and M_Y from 0 to $M_X - 5$ GeV. The efficiencies for XX and XY production for the case $M_Y = 0$ are found to be identical within statistical errors to the efficiencies obtained using the OPAL excited neutrino Monte Carlo generator described in [21].

All the above Monte Carlo samples were processed through the OPAL detector simulation [22].

3 Event Selection Description

3.1 Topology A: Events with one or two photons and invisible particle(s)

Events are selected as having one or two photon candidates if they satisfy the following criteria based on previous OPAL analyses of photonic events with missing energy [1, 3, 23]:

- **Charged track veto.** Events are required to have no tracks with 20 or more jet chamber hits assigned to them, reconstructed in the central detector.
- **Angular acceptance and minimum energy.** An event is considered to contain a photon candidate if the primary electromagnetic cluster (that with the highest deposited energy in the barrel and endcap calorimeters) is in the region $|\cos\theta| < 0.7$ and has a scaled energy, x_γ , that exceeds 0.2. Events are considered to have more than one photon if additional electromagnetic clusters are found in the barrel or endcap calorimeter ($|\cos\theta| < 0.984$) having deposited energy exceeding 300 MeV. Acceptance for events with two photons is desirable in order to increase the efficiency for doubly radiative neutrino production, and so reduce the sensitivity to the modelling of that process.
- **Cluster extent.** The primary electromagnetic cluster combined with any clusters contiguous with it must not extend more than 250 mrad (equivalent to more than six lead-glass blocks) in the polar or azimuthal directions. It must also consist of at least two blocks.
- **Coil conversion seen in TOF system.** The primary electromagnetic cluster must be matched within 50 mrad in azimuthal angle by a good quality TOF counter signal produced by the photon converting in the coil in front of the TOF. The measured arrival time of the photon at the TOF must be within 20 ns of the expected time for a photon originating from the interaction point.
- **Forward calorimeter veto.** The total energy deposited in each forward calorimeter must be less than 2 GeV.
- **Gamma-catcher veto.** The most energetic gamma-catcher cluster must have an energy of less than 5 GeV. The forward calorimeter veto and gamma-catcher veto serve to ensure that photon candidate events are not accompanied by any event activity in the forward regions.
- **Muon veto.** Events are rejected if there are any muon track segments reconstructed in the barrel or endcap muon chambers, or in the barrel, endcap or pole-tip hadron calorimeters. Events are also rejected if three or more of the outer 8 layers of the barrel hadron calorimeter have strips hit in any 45° azimuthal road. The muon veto is used primarily to remove cosmic ray background.

Background from $e^+e^- \rightarrow \gamma\gamma(\gamma)$ is rejected if any of the following criteria are satisfied for events with a second cluster:

- The total energy of the two clusters exceeds 90% of the centre-of-mass energy.
- The acoplanarity angle of the two clusters¹, ϕ_{acop} , is less than 2.5°.
- The missing momentum vector calculated from the two clusters satisfies $|\cos\theta_{\text{miss}}| > 0.9$.
- A third electromagnetic cluster is detected with deposited energy exceeding 300 MeV.

¹Defined as 180° minus the opening angle in the transverse plane.

3.2 Topology B: Events with an acoplanar photon pair and invisible particle(s)

The event selection for this topology is also based on the previous OPAL analyses described in references [24] and [1]. The selection criteria for topology B are identical for those of topology A except for the following two requirements:

- **Angular acceptance and minimum energy.** Candidate events are required to contain two electromagnetic clusters in the calorimeter, both having deposited energy exceeding 1.5 GeV and detected in the region $|\cos\theta| < 0.7$. Following [3], the experimental requirement on deposited energy exceeding 1.5 GeV corresponds to an effective minimum photon energy of 1.75 GeV. The cluster with the higher energy must pass the cluster extent criteria of topology A.
- **Coil conversion seen in TOF system.** At least one electromagnetic cluster must be matched within 50 mrad in azimuthal angle by a good quality TOF counter signal. The measured arrival time of the photon at the TOF must be within 20 ns of the expected time for a photon originating from the interaction point.

The restricted angular acceptance for the two photons in topology B not only discriminates against forward-peaked background, it also ensures precise measurement of the photon energies and helps ensure that time-of-flight information is available to check that the photons are consistent with originating from the interaction point. Background events, coming principally from $e^+e^- \rightarrow \gamma\gamma(\gamma)$, are rejected if any of the same four veto conditions described in topology A are satisfied.

4 Results

4.1 Topology A

After applying the selection criteria of topology A to the data sample, 11 events are selected. From the Monte Carlo we expect a Standard Model signal from $e^+e^- \rightarrow \nu\bar{\nu}\gamma(\gamma)$ of 16.1 ± 0.3 events. The selection efficiency for this Standard Model process is (69 ± 1) % for generated events within the kinematic acceptance (i.e. at least one photon with $x_\gamma > 0.2$ and $|\cos\theta| < 0.7$). Most of the inefficiency arises when a photon either converts in the tracking volume, or does not convert until it enters the lead glass calorimeter. In the former case, such events are vetoed by the presence of charged tracks and in the latter case it is unlikely that a TOF hit will be associated with the electromagnetic cluster.

Here and throughout the paper the quoted errors on efficiencies include estimates of the systematic errors which are small compared to the statistical errors on the measurements. The expected $e^+e^- \rightarrow \nu\bar{\nu}\gamma(\gamma)$ contribution can be divided into 13.5 ± 0.3 single photon events and 2.6 ± 0.1 two photon events (see Table 1). In the data all 11 events are single photon events. The expected contributions from all Standard Model background processes are estimated to be negligible (less than 0.1 events expected). Beam-related, cosmic ray and instrumental background contributions are also negligible. With 11 observed events and correcting for the selection efficiency, we obtain a cross-section for $e^+e^- \rightarrow \nu\bar{\nu}\gamma(\gamma)$ within the kinematic acceptance of topology A of 1.6 ± 0.5 pb, consistent with the Standard Model prediction of 2.3 pb. This measured cross-section, along with the same measurements by OPAL at $\sqrt{s}=130$ GeV and 136 GeV are plotted in Fig. 1. The curve shows the predicted Standard Model cross-section.

The scaled energy distribution of the most energetic photon for events found in the data is plotted along with the expected Standard Model signal $e^+e^- \rightarrow \nu\bar{\nu}\gamma(\gamma)$ and background contributions in Fig. 2a. In the figure, the threshold for the x_γ cut has been lowered to 0.025 (about 2 GeV) to

show the expected background contributions at low photon energy. There is good agreement between data and Monte Carlo predictions both for the background dominated low x_γ region and in the $x_\gamma > 0.2$ signal region. That the 11 selected events in the data are consistent with the expectation for $e^+e^- \rightarrow \nu\bar{\nu}\gamma(\gamma)$ can also be seen in the distribution of the mass recoiling against the photon (or two-photon system) as shown in Fig. 2b. One expects a peak in the recoil mass at M_Z , since the $\nu\bar{\nu}$ predominantly comes from the decay of a Z^0 .

We now apply a cut on the recoil mass of $M_{\text{rec}} < 75$ GeV and require only one photon. These cuts remove most of the Standard Model $e^+e^- \rightarrow \nu\bar{\nu}\gamma(\gamma)$ events, providing a nearly background-free kinematic region to look for possible new physics processes. The number of events from $e^+e^- \rightarrow \nu\bar{\nu}\gamma(\gamma)$ expected from the Monte Carlo is reduced from 16.1 to 0.09 after the first cut and further reduced to 0.04 after the second. No events survive the first cut in the data. We can derive a 95% CL upper limit of 0.44 pb for single photon production within this kinematic region. This limit uses the expected polar angle and energy distributions for the process $e^+e^- \rightarrow \nu\bar{\nu}\gamma(\gamma)$ but is not very sensitive to the shape of these distributions. The systematic error is incorporated into all limits quoted in this paper using the method described in [25].

After applying the topology A selection with the additional two cuts described above, we obtain the efficiency for selecting events from the process $e^+e^- \rightarrow XY, X \rightarrow Y\gamma$ ($M_Y \approx 0$), which varies from 14% for $M_X = 80$ GeV to 56% for $M_X = 160$ GeV as shown in Table 2. Based on these efficiencies and on no observed events in the data, we can set an upper limit on the cross-section times photonic branching ratio, $\sigma_{XY} \times \text{BR}(X \rightarrow Y\gamma)$, as a function of M_X , as shown in Fig. 3a. This limit applies to the supersymmetry process of $\tilde{\chi}_2^0\tilde{\chi}_1^0$ production where $\tilde{\chi}_1^0$ is massless and also to the case of single production of excited neutrinos ($e^+e^- \rightarrow \nu^*\nu, \nu^* \rightarrow \nu\gamma$). Further excited neutrino results obtained using these data as well as other excited lepton results from OPAL can be found in [21].

4.2 Topology B

After applying the selection criteria of topology B to the data, no events remain, consistent with the expectation for the Standard Model process $e^+e^- \rightarrow \nu\bar{\nu}\gamma\gamma$ of 0.93 ± 0.08 events. The expected number of events from other processes and instrumental backgrounds is negligible. The selection efficiency for this process is (74 ± 3) % for those events generated within the kinematic acceptance of topology B (i.e., both photons having $E_\gamma > 1.75$ GeV and $|\cos\theta| < 0.7$). Therefore we set an upper limit on the cross-section within this kinematic acceptance for acoplanar photon pair production of 0.41 pb at 95% CL. This limit uses the expected polar angle and energy distributions for the process $e^+e^- \rightarrow \nu\bar{\nu}\gamma\gamma$ but is not very sensitive to the shape of these distributions. The expected cross-section for $e^+e^- \rightarrow \nu\bar{\nu}\gamma\gamma$ is 0.12 pb.

The results of this topology are also interpreted in the context of pair production of particle X and subsequent decay $X \rightarrow Y\gamma$. For the general case of arbitrary values of M_Y , the efficiency of the analysis over the full angular acceptance exceeds 26% for $M_X > 40$ GeV and $M_Y < M_X - 5$ GeV. For these ranges of M_X and M_Y , the result leads to a cross-section upper limit of 1.2 pb at 95% CL over the full acceptance. For the specific case of $M_Y \approx 0$, relevant to excited neutrinos and light gravitinos, we try to reduce further the expected background. In Fig. 4a we plot the energy of the less energetic photon (E_2) against the energy of the more energetic photon (E_1) for the Standard Model $e^+e^- \rightarrow \nu\bar{\nu}\gamma\gamma$ Monte Carlo events. The distribution shows that a large fraction of the expected events contain one very energetic photon and one soft photon, and that the sum of the photon energies is likely to be close to 55 GeV ($0.34\sqrt{s}$) which is the energy expected for production of a real Z^0 accompanied by a low mass di-photon system. The line represents $E_1 + E_2 = 0.4\sqrt{s}$ and we choose the region above this line as the search region for new physics signals because it is kinematically unlikely that events arising from real Z^0 production populate this region. One expects 0.04 ± 0.02 events in this region from the Standard Model process $e^+e^- \rightarrow \nu\bar{\nu}\gamma\gamma$.

Figure 4(b)-(d) shows the expected E_2 versus E_1 distributions for XX production with M_X of 55, 70 and 80 GeV, respectively, and $M_Y = 0$ GeV. The defined search region has a high acceptance for this signal, especially close to the kinematic limit, while reducing the Standard Model expectation by more than an order of magnitude. The efficiencies for XX production and expected Standard Model backgrounds are listed in Table 3 for both the standard selection and after including the energy sum requirement. Based on the latter efficiencies within the full acceptance (typically 25%) and given no observed events in the data, we set 95% CL upper limits on the cross-section for XX production multiplied by the photonic decay branching ratio squared, $\sigma_{XX} \times \text{BR}^2(X \rightarrow Y\gamma)$, for massless Y. These limits are shown in Fig. 3b. For $M_X = 50$ GeV, this limit on $\sigma_{XX} \times \text{BR}^2(X \rightarrow Y\gamma)$ is 1.5 pb and for $M_X = 75$ GeV it is 1.0 pb. For example, this can be compared with the case of a light gravitino as described in [12], for which a cross-section of about 1 pb is expected for $M_{\tilde{\chi}_1^0} = 50$ GeV.

As described above, the efficiencies over the full angular range have been calculated with isotropic angular distributions for production and decay of X. We have examined the validity of this assumption based on the angular distributions calculated for photino pair production in [10]. For models proposed in [11], the production angular distributions are more central and so this assumption is conservative. For an extreme case, namely a $1 + \cos^2 \theta$ production angular distribution, appropriate to t-channel exchange of a very heavy particle [10], the relative efficiency reduction would be at most 15%. We have evaluated the efficiency with zero decay length for X; efficiencies are unaffected if the decay length is much less than the inner radius of the barrel electromagnetic calorimeter (2.5 m).

5 Conclusions

We have searched for photonic events with large missing energy in two different and complementary topologies from data taken at $\sqrt{s} = 161$ GeV. The search is sensitive to several types of new physics in e^+e^- collisions producing invisible particles that escape detection.

In the topology A selection which requires events to have at least one photon with $x_\gamma > 0.2$ and $|\cos \theta| < 0.7$, 11 events are observed in the data compared to an expected contribution from the Standard Model process $e^+e^- \rightarrow \nu\bar{\nu}\gamma(\gamma)$ of 16.1 ± 0.3 events. This corresponds to a cross-section for $e^+e^- \rightarrow \nu\bar{\nu}\gamma(\gamma)$ of 1.6 ± 0.5 pb within the kinematic acceptance of topology A, consistent with the Standard Model prediction of 2.3 pb. By considering only events with a single photon and with a recoil mass below 75 GeV, based on no observed events, we determine a 95% CL upper limit for the cross-section of 0.44 pb. In addition we set an upper limit on the cross-section times photonic branching ratio for the process $e^+e^- \rightarrow XY, X \rightarrow Y\gamma, M_Y \approx 0$ as a function of M_X . This limit is of particular interest for the case of new physics processes producing single photons such as for the supersymmetry process $e^+e^- \rightarrow \tilde{\chi}_2^0\tilde{\chi}_1^0 \rightarrow \tilde{\chi}_1^0\tilde{\chi}_1^0\gamma$ and for single production of excited neutrinos [21].

The topology B selection which requires events to have two photons, each with energy exceeding 1.75 GeV and $|\cos \theta| < 0.7$, finds no events passing all cuts. This is consistent with the prediction for the Standard Model process $e^+e^- \rightarrow \nu\bar{\nu}\gamma\gamma$ of 0.93 ± 0.08 events. We set an upper limit on the cross-section for acoplanar photon pair production within the kinematic acceptance of topology B of 0.41 pb at 95% CL. We also set a 95% CL upper limit on the cross-section times photonic branching ratio squared of 1.2 pb for the process $e^+e^- \rightarrow XX, X \rightarrow Y\gamma$ for $M_X > 40$ GeV and $M_Y < M_X - 5$ GeV. This limit is of interest for the case of pair produced new particles which decay to undetectable massive particles and photons. By requiring a minimum total energy for the two photons, the already small $e^+e^- \rightarrow \nu\bar{\nu}\gamma\gamma$ contribution is made negligible and we derive a 95% CL upper limit for the cross-section times branching ratio squared for XX production as a function of M_X where $M_Y \approx 0$. This limit is of particular interest for new physics processes producing acoplanar photon pairs and undetectable massless particles, for example, pair produced neutralinos, where the neutralino decays into a photon and a light gravitino, or pair produced excited neutrinos [21].

Acknowledgements

We particularly wish to thank the SL Division for the efficient operation of the LEP accelerator at the new energy of $\sqrt{s} = 161$ GeV and for their continuing close cooperation with our experimental group. We thank our colleagues from CEA, DAPNIA/SPP, CE-Saclay for their efforts over the years on the time-of-flight and trigger systems which we continue to use. In addition to the support staff at our own institutions we are pleased to acknowledge the

Department of Energy, USA,

National Science Foundation, USA,

Particle Physics and Astronomy Research Council, UK,

Natural Sciences and Engineering Research Council, Canada,

Israel Science Foundation, administered by the Israel Academy of Science and Humanities,

Minerva Gesellschaft,

Japanese Ministry of Education, Science and Culture (the Monbusho) and a grant under the Monbusho International Science Research Program,

German Israeli Bi-national Science Foundation (GIF),

Bundesministerium für Bildung, Wissenschaft, Forschung und Technologie, Germany,

National Research Council of Canada,

Hungarian Foundation for Scientific Research, OTKA T-016660, and OTKA F-015089.

References

- [1] OPAL Collab., G. Alexander et al., Phys. Lett. **B377** (1996) 222.
- [2] OPAL Collab., G. Alexander et al., CERN-PPE/96-094, to be published in Phys. Lett. B.
- [3] OPAL Collab., R. Akers et al., Z. Phys. **C65** (1995) 47.
- [4] L3 Collab., B. Adeva et al., Phys. Lett. **B275** (1992) 209;
L3 Collab., O. Adriani et al., Phys. Lett. **B292** (1992) 463;
ALEPH Collab., D. Buskulic et al., Phys. Lett. **B313** (1993) 520;
DELPHI Collab., P. Abreu et al., CERN-PPE/96-03, submitted to Z. Phys. **C**.
- [5] MAC Collab., W.T. Ford et al., Phys. Rev. **D33** (1986) 3472;
H. Wu, Ph.D Thesis, Univ. Hamburg, 1986;
CELLO Collab., H.-J. Behrend et al., Phys. Lett. **B215** (1988) 186;
ASP Collab., C. Hearty et al., Phys. Rev. **D39** (1989) 3207;
VENUS Collab., K. Abe et al., Phys. Lett. **B232** (1989) 431;
TOPAZ Collab., T. Abe et al., Phys. Lett. **B361** (1995) 199.
- [6] ALEPH Collab., D. Buskulic et al., Phys. Lett. **B384** (1996) 333;
L3 Collab., M. Acciarri et al., Phys. Lett. **B384** (1996) 323;
DELPHI Collab., P. Abreu et al., Phys. Lett. **B380** (1996) 471.
- [7] L3 Collab., M. Acciarri et al., Phys. Lett. **B346** (1995) 190 and Phys. Lett. **B350** (1995) 109.
- [8] H.E. Haber and D. Wyler, Nucl. Phys. **B323** (1989) 267;
S. Ambrosanio and B. Mele, Phys. Rev. **D53** (1996) 2541.
- [9] S. Ambrosanio et al., Phys. Rev. Lett. **76** (1996) 3498 and hep-ph/9607414.
- [10] J. Ellis and J.S. Hagelin, Phys. Lett. **B122** (1983) 303.

- [11] S. Dimopoulos et al., Phys. Rev. Lett. **76** (1996) 3494;
D.R. Stump, M. Wiest, C.P. Yuan, Phys. Rev. **D54** (1996) 1936;
C.Y. Chang and G.A. Snow, UMD/PP/97-57.
- [12] J.L. Lopez and D.V. Nanopoulos, hep-ph/9608275;
J.L. Lopez, D.V. Nanopoulos, A. Zichichi, hep-ph/9609524.
- [13] OPAL Collab., K. Ahmet et al., Nucl. Instrum. Methods **A305** (1991) 275;
P.P. Allport et al., Nucl. Instrum. Methods **A324** (1993) 34;
P.P. Allport et al., Nucl. Instrum. Methods **A346** (1994) 476;
B.E. Anderson et al., IEEE Transactions on Nuclear Science **41** (1994) 845.
- [14] G. Montagna et al., Nucl. Phys. **B452** (1996) 161;
G. Montagna, O. Nicosini and F. Piccinini, FNT/T-96/1, to be published in Comp. Phys. Comm.
- [15] F.A. Berends and R. Kleiss, Nucl. Phys. **B186** (1981) 22.
- [16] S. Jadach, W. Placzek and B. F. L. Ward, University of Tennessee preprint, UTHEP 95-1001 (unpublished).
- [17] D. Karlen, Nucl. Phys. **B289** (1987) 23.
- [18] S. Jadach et al., Comp. Phys. Comm. **66** (1991) 276.
- [19] J. A. M. Vermaseren, Nucl. Phys. **B229** (1983) 347.
- [20] S. Katsanevas and S. Melachronios, CERN/96-01, Vol.2 (1996) 328.
- [21] OPAL Collab., K. Ackerstaff et al., CERN-PPE/96-138, submitted to Phys. Lett. B.
- [22] J. Allison et al., Nucl. Instrum. Methods **A317** (1992) 47.
- [23] OPAL Collab., G. Alexander et al., Phys. Lett. **B377** (1996) 273.
- [24] OPAL Collab., P.D. Acton et al., Phys. Lett. **B311** (1993) 391.
- [25] R. D. Cousins and V. L. Highland, Nucl. Instrum. Methods **A320** (1992) 331.

Process	1 photon	1 or 2 photons	1 photon and $M_{\text{rec}} < 75$ GeV	1 or 2 photons and $M_{\text{rec}} < 75$ GeV
Data	11	11	0	0
$e^+e^- \rightarrow \nu\bar{\nu}\gamma(\gamma)$	13.5 ± 0.3	16.1 ± 0.3	0.04 ± 0.02	0.09 ± 0.02

Table 1: Topology A selection: Number of events observed in the data and expected number of events from the process $e^+e^- \rightarrow \nu\bar{\nu}\gamma(\gamma)$ for an integrated luminosity of 10.0 pb^{-1} .

M_X (GeV)	Efficiency in % for topology A selection	Efficiency in % for topology A with 1 photon and $M_{\text{rec}} < 75$ GeV
80	42 ± 2	14 ± 1
110	40 ± 2	20 ± 1
130	42 ± 2	33 ± 1
150	53 ± 2	50 ± 2
160	56 ± 2	56 ± 2

Table 2: Topology A selection efficiency as a function of mass for the process $e^+e^- \rightarrow XY$, $X \rightarrow Y\gamma$, and $M_Y \approx 0$.

Process	standard selection		standard selection and $E_1 + E_2 > 0.4\sqrt{s}$	
	effic. in %	no. of events	effic. in %	no. of events
Data		0		0
$e^+e^- \rightarrow \nu\bar{\nu}\gamma\gamma$	74 ± 3	0.93 ± 0.08		0.04 ± 0.02
$M_X = 45$ GeV	32 ± 1		20 ± 1	
$M_X = 55$ GeV	33 ± 1		22 ± 1	
$M_X = 70$ GeV	31 ± 1		24 ± 1	
$M_X = 75$ GeV	35 ± 2		31 ± 1	
$M_X = 80$ GeV	33 ± 1		33 ± 1	

Table 3: Topology B selection: Efficiencies and expected number of events for an integrated luminosity of 10.0 pb^{-1} . The efficiency for $e^+e^- \rightarrow \nu\bar{\nu}\gamma\gamma$ is defined relative to the kinematic region mentioned in the text. The last five rows of the table give the efficiency for selecting events of the type $e^+e^- \rightarrow XX$, $X \rightarrow Y\gamma$ and $M_Y \approx 0$, for varying M_X .

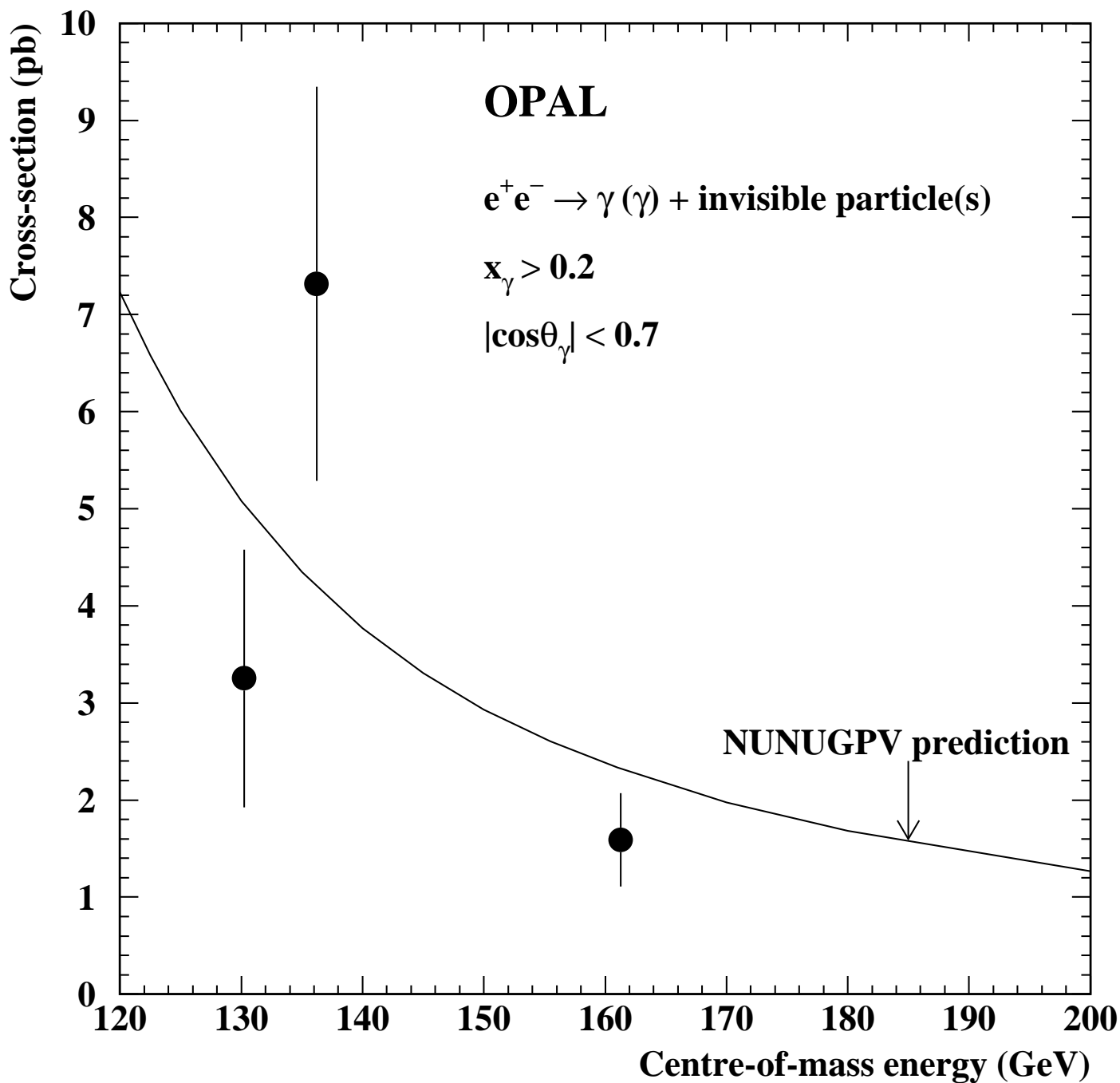


Figure 1: The measured cross-section for $e^+e^- \rightarrow \gamma(\gamma) + \text{invisible particle(s)}$ versus centre-of-mass energy. The data points with error bars are OPAL measurements from this paper and from the analysis at centre-of-mass energies of 130 and 136 GeV. The curve is the Standard Model prediction for the process $e^+e^- \rightarrow \nu\bar{\nu}\gamma(\gamma)$.

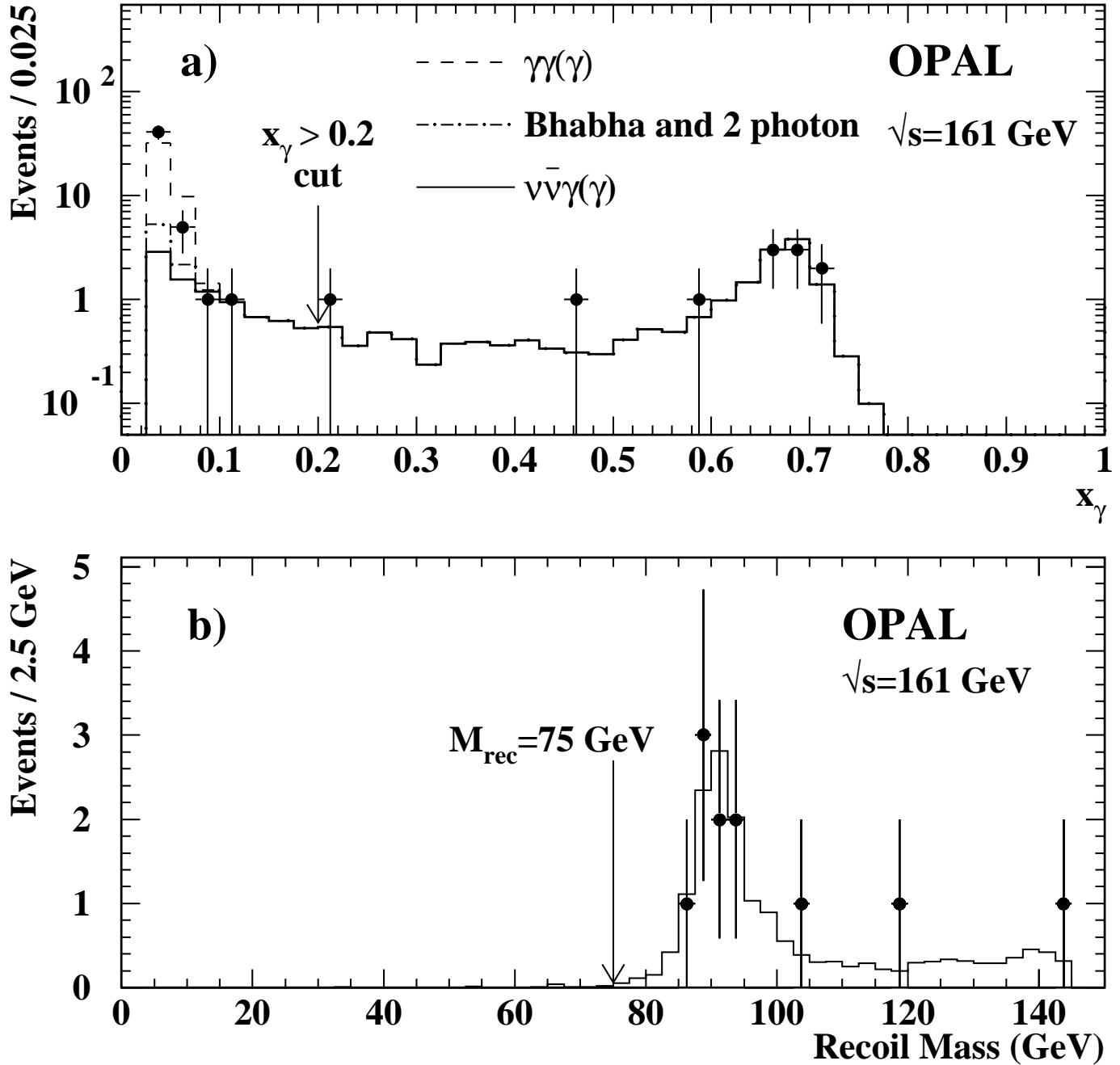


Figure 2: a) The x_γ distribution for the most energetic photon in events selected by topology A without the x_γ cut in order to show the expected background contributions at low x_γ . The data are the points with error bars, the solid line is the expected contribution from $e^+e^- \rightarrow \nu\bar{\nu}\gamma(\gamma)$ and the broken lines are the additional contribution from other Standard Model backgrounds. The Monte Carlo contributions are normalised to the 10.0 pb^{-1} of the data. b) The recoil mass distribution for selected events in topology A. The points with error bars are the data and the histogram is the expectation from the $e^+e^- \rightarrow \nu\bar{\nu}\gamma(\gamma)$ Monte Carlo normalised to the 10.0 pb^{-1} of the data.

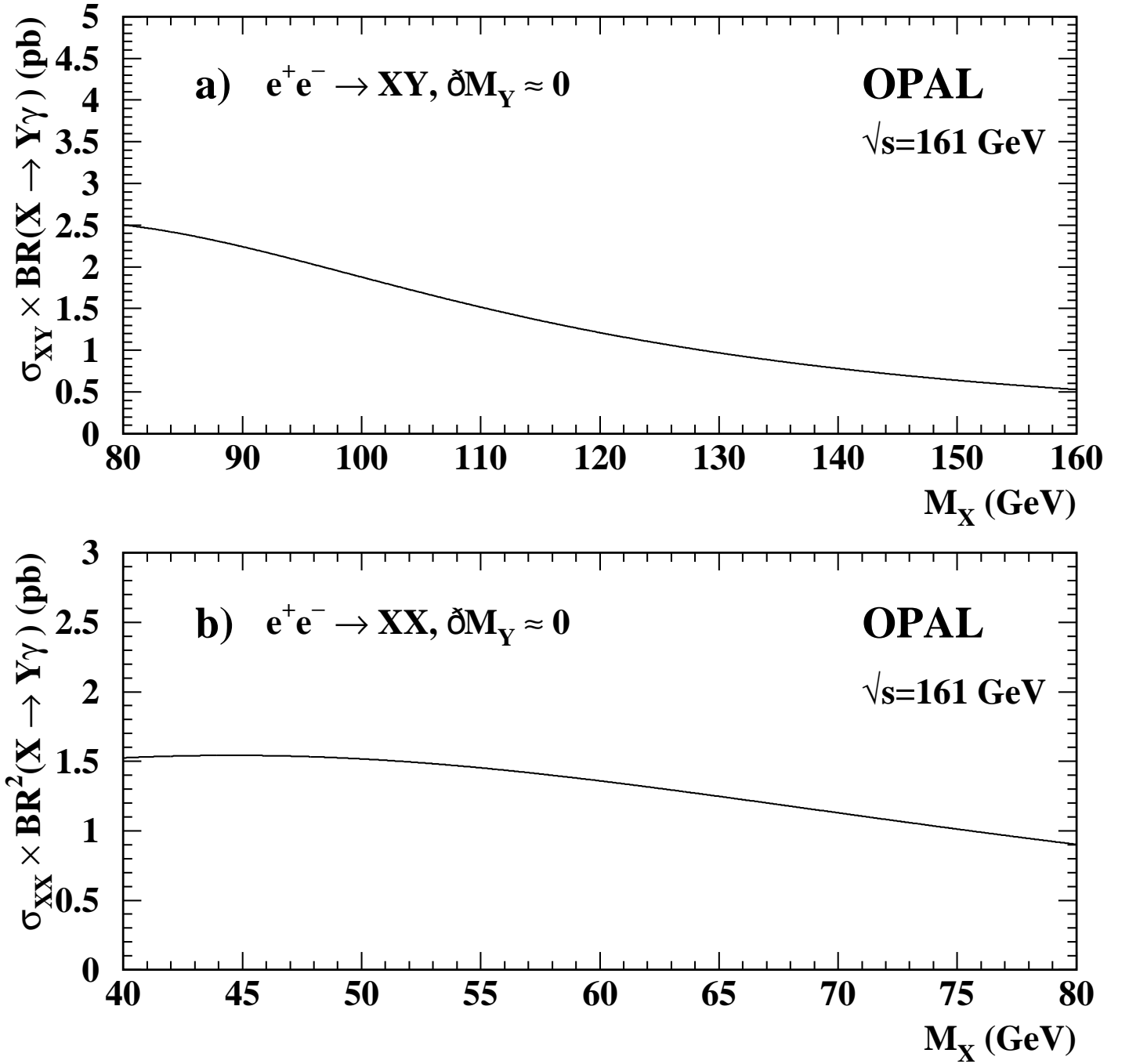


Figure 3: a) The 95% CL upper limit on the cross-section times the photonic branching ratio for the process $e^+e^- \rightarrow XY$, $X \rightarrow Y\gamma$ with $M_Y \approx 0$, versus M_X . This limit uses the topology A selection for one photon only and $M_{\text{rec}} < 75 \text{ GeV}$. b) The 95% CL upper limit on the cross-section times the photonic branching ratio squared for the process $e^+e^- \rightarrow XX$, $X \rightarrow Y\gamma$ with $M_Y \approx 0$, versus M_X . This limit uses the topology B selection with the $E_1 + E_2 > 0.4\sqrt{s}$ cut.

OPAL

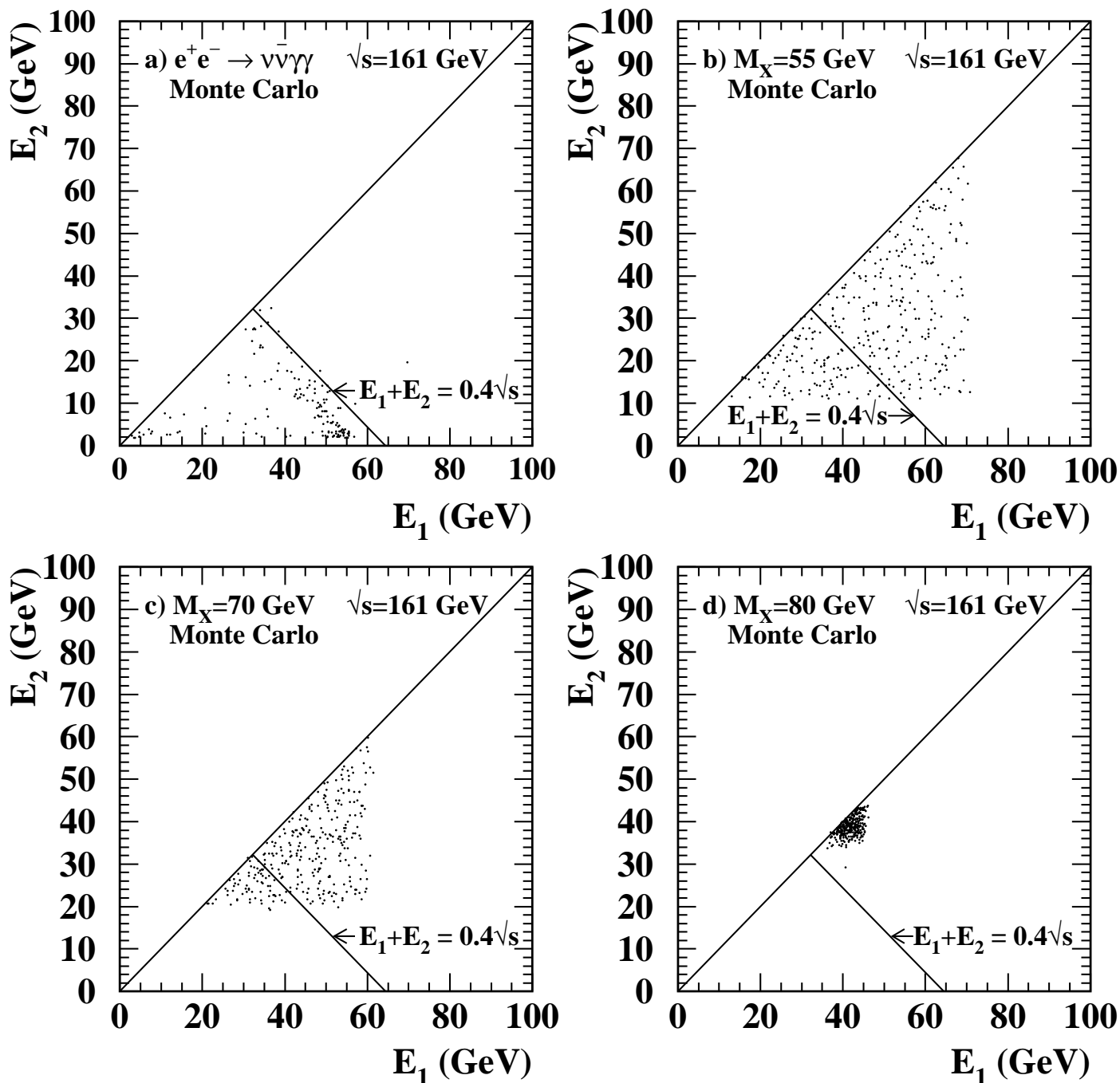


Figure 4: The energies of the lower versus the higher energy photon for events passing the topology B selection. No data events are selected for this topology. a) $e^+e^- \rightarrow \nu\bar{\nu}\gamma(\gamma)$ Monte Carlo events corresponding to a luminosity of 1.5 fb^{-1} . b-d) Events of the type $e^+e^- \rightarrow XX$, $X \rightarrow Y\gamma$ with $M_Y \approx 0$. The events shown correspond to 1000 events generated for each of three mass values for X: b) $M_X = 55$ GeV, c) $M_X = 70$ GeV, d) $M_X = 80$ GeV.